Supporting Information

Bierne et al. 10.1073/pnas.0901259106

SI Materials and Methods

Cell Lines and Antibodies. The C3SV40 cells were human fibroblastic cells established from a skin biopsy specimen from a healthy male adult and transformed with SV40T, as described previously (1). C3SV40 cells were grown in RPMI 1640 (Gibco) supplemented with 10% FCS (Gibco). The other cells lines used were obtained from ATCC (www.atcc.org) and grown in accordance with ATCC recommendations. They include embryonic kidney cells HEK293 (ATCC#CRL-1573), placental cells JEG-3 (ATCC#HTB-36), intestinal Lovo cells (ATCC#CCL-229), human diploid fibroblasts IMR90 (ATCC#CCL-186) and WI-38 (ATCC#CCL75), and mouse fibroblasts Swiss 3T3 (ATCC#CCL-92). All cells were cultured at 37 °C with 5% or 10% CO_2. The primary antibodies used were as follows: acetyl H4 (06–598; Millipore), H3K27me3 (07–449; Millipore), H3K9me3 (07–442; Millipore), HDAC5 (Abcam ab1439 for IP and Active Motif 40970 for ChIP), MBD1 (Abcam ab3753), SP1 (Abcam ab13370), HP1α (clone 2HP-1H5 for immunofluorescence and clone 2HP-2G9 for immunohistochemistry; Euromedex), AP2 (Abcam ab61), V5 and V5-HRPO (Invitrogen), and GST (Novagen). The anti-BAHD1 was generated against a peptide corresponding to the last 17 amino acids of BAHD1 and was affinity-purified.

Plasmids and Cloning Strategies. To clone *BAHD1* cDNA, total RNA was purified from 1×10^7 JEG3 or HEK293 cells using the Qiagen RNeasy Mini Kit, and cDNAs were amplified using the SuperScript III First-Strand synthesis system and Platinum Taq polymerase high fidelity (both from Invitrogen) according to the manufacturer's protocol. The PCR fragments were directly subcloned, using a directional topoisomerase cloning system, into the mammalian expression vector pcDNA3.1/V5-His-TOPO (Invitrogen), leading to pcV5-BAHD1 vectors. Both sequences were identical to the published sequence (accession number NM_014952; gene ID 22893) with one D182H modification corresponding to a single nucleotide polymorphism described previously (http://www.ncbi.nlm.nih-.gov/projects/SNP; rs17856679). The control plasmid pcV5-CFP was constructed by inserting the sequence encoding the CFP from pE-mCFP-N1 (3) in pcDNA3.1/V5-His-TOPO. The plasmid pcV5-BAHD1 was used to amplify and subclone full-length BAHD1 into pB27 (Hybrigenics), pE-citrine-N1 (4), or pSG424-GALM, or only the sequence encoding the last 193 amino acids of BAHD1 (aa 587–780) into pET41a(+) (Novagen), with the primers and restriction enzymes indicated below. pE-citrine-N1 encodes cYFP, a variant of YFP with better photostability than other YFP variants (4). The pSG424-GALM vector, which allows the expression of GAL4 (1–147) fusions in mammalian cells, is derived from pSG424 (5) modified to contain additional restriction sites (NdeI/NcoI/PstI/BsteEII) in the polylinker cloning site. pGEX-MBD1 and pGAL-MBD1 were generated by PCR amplification of human MBD1 cDNA (splice variant 3) from an EST clone (IMAGE:5432943) in vector pGEX2T (Amersham Pharmacia) or pSG424-GALM. pGEX-HP1α and pGAL-HP1α were generated by PCR amplification of human HP1α. pMMTV-Luc was constructed by cloning a GAL-binding site in the SacI site of the MMTV promoter in pFc31Luc (6). The pG5TK-Luc was a kind gift from J. G. Judde, and the plasmid pcDNA3 encoding GFP-PML (variant IV) was a kind gift from O. Bischof. All constructs were verified by double-strand sequencing. The plasmids and oligonucleotides used are listed in Table S4 .

Identification of BAHD1 Interactors by Yeast Two-Hybrid Screening and Construction of an Interaction Network. The bait construct was *BAHD1* cloned in pB27, a Y2H vector optimized by Hybrigenics (http:/www. hybrigenics.com). pB27-*BAHD1* was transformed in the L40DGAL4 yeast strain (7), and Y2H screening was performed by Hybrigenics. A human placenta random-primed cDNA library (RP4) transformed into the Y187 yeast strain and containing 10 million independent fragments was used for mating. High mating efficiency was ensured by using a specific mating method (7). The screen was first performed on a small scale, to adapt the selective pressure to the intrinsic property of the bait. Neither toxicity nor autoactivation of the bait was observed. Then the full-scale screen was performed under conditions ensuring that a minimum of 50 million interactions were tested, to cover 5 times the primary complexity of the yeast-transformed cDNA library (8). A total of 54.96 million interactions were actually tested. After selection on medium lacking leucine, tryptophane, and histidine, positive clones were chosen, and the corresponding prey fragments were amplified by PCR and sequenced at their 5′ and 3′ junctions. Sequences were then filtered and contiged as described previously (9) and compared with the latest release of the GenBank database using BLAST (10). For all nuclear preys, the predicted interaction was weak, as identified through a unique prey fragment or multiple identical fragments.

To generate the BAHD1 interactome, we used data from our whole human genome Y2H screen, as well as data obtained in a Y2H screen of pairwise interactions between 7,200 human protein-encoding genes (11), in which BAHD1 partners, such as MDFI and DVL3, were found. All BAHD1 interactors were uploaded in the Ingenuity Pathways Analysis software (www.ingenuity.com) to create a network of direct protein–protein interactions. All proteins were also checked for interactors, one-by-one, in the Human Protein Reference Database (http://www.hprd.org).

Transient Transfections With Plasmids or Oligofection With siRNA Duplexes. Transient transfections were performed as described previously (12) using lipofectamine 2000 or LTX (Invitrogen) according to the manufacturer's protocol. To knock down expression of *BAHD1*, HEK293 was transfected with chemically synthesized siRNAs (Ambion) using lipofectamine RNAi max (Invitrogen) following the manufacturer's instructions. A combination of 3 different siRNA duplexes (in microarray experiments) or individual siRNA BAHD1 1 or 2 (in qRT-PCR assays) was used.

The silencer negative control 1 siRNA (Ambion #4611) was used as a control. The silencing efficiency of these siRNAs was examined by RT-PCR or qRT-PCR (see Table S5) at 72 h posttransfection. The RT-PCR procedure used a SuperScript One-Step RT-PCR (Invitrogen) with serial dilutions of the RNA template, according to the manufacturer's protocol, and the following primers: for *BAHD1*, forward, atgcttcctgagggcaagctgtcc; reverse, gtaagtgctcaggtctgtaatacc; for *GAPDH*, forward, gtcgtattgggcgcctggtcac; reverse, cacgacgtactcagcgccagca. siRNA treatment did not alter cell morphology or growth.

Immunofluorescence Analysis, Live Cell Imaging, and Image Processing. Cells were fixed for 20 min at room temperature with 3% or 4% paraformaldehyde in PBS, permeabilized with 0.4% or 0.5% Triton X-100 in PBS for 4 min at room temperature, blocked in PBS containing 1% BSA (Sigma), and, when indicated, incu-

bated with primary antibodies for 1 h and then with secondary antibodies for 1 h. The secondary antibodies used were Alexa 488–conjugated (Molecular Probes) or Cy3-, Texas red–, or Cy5-conjugated (Jackson IR) goat anti-mouse or anti-rabbit IgGs antibodies. Nuclei were visualized in phase contrast and with DAPI. The preparations were examined with a Zeiss Axiovert 200M epifluorescence microscope, connected to a cooled CCD camera (CoolSNAP$_{HQ}$; Photometrics), or with a Zeiss LSM 510 confocal laser scanning microscope. Images were acquired with apochromat 63× or 100× (NA 1.4) objective lenses and processed using MetaMorph version 6.1 (Universal Imaging) or Zeiss LSM Image software. For live cell imaging, images were acquired with a microscope equipped with a temperature-controlled stage and an objective heater (Biotechs). Fluorescent illumination was driven by an ultra–high-speed wavelength switcher (Lamda DG4; Sutter Instrument) equipped with a 175-W xenon arc lamp and excitation filters for YFP (Chroma Technology). Emission filters were selected using a high-speed Lamda 10 filter wheel (Sutter Instrument). For 3D reconstruction of BAHD1 foci in the nucleus, HEK293 cells expressing V5-BAHD1 were fixed, stained with DAPI and V5 antibody, and analyzed with a Zeiss LSM-510 confocal microscope. Stacks of confocal images were deconvoluted with Huygens software (Scientific Volume Imaging) and processed with OsiriX software (13). DAPI staining was used to define the nucleus volume. The V5 staining was threshold compared with the V5 staining in untransfected HEK293 cells.

RNA FISH. A DNA probe detecting Xist RNA was nick-translated using plasmid G1A (from the fourth intron to the 3′ end of the human *Xist* gene), a Nick-translation kit (Abbot), and spectrum-red-dUTP (Abbot). After the addition of human COT-1 (Invitrogen) and tRNA (Roche), the labeled probe was precipitated with ethanol, resuspended in formamide (Sigma), and denatured for 10 min at 80 °C. Cell cultures on coverslips were fixed in 3% paraformaldehyde for 10 min and permeabilized with 1× PBS/0.5% Triton X-100 for 4 min. Cells were blocked with PBS, 1% BSA, tRNA, and RNAguard (Amersham), and then dehydrated in ethanol. Cells were then incubated overnight at 37 °C in a hybridization mixture containing denaturated probe, 0.75% BSA, 2× SSC, 10% dextran sulfate, and vanadyl ribonucleoside complex (Biolabs). After washes in 2× SSC/50% formamide, in 2× SSC, and then in 1× SSC, coverslips were mounted on slides with antifading solution containing DAPI.

Transmission Electron Microscopy. HEK293 cells were transfected with the YFP-BAHD1 expression vector and then either directly fixed or sorted by FACS to enrich for YFP-BAHD1–positive cells (at 488-nm excitation) and expanded overnight before fixation. Both procedures gave similar results, except that the sorted cells appeared deformed and rounded. Untransfected and transfected cells were fixed in 2.5% glutaraldehyde and postfixed with 1% osmium tetroxide in 0.1 M cacodylate buffer (pH 7.4). The cells were stained en bloc with 2% uranyl acetate in 30% methanol, then dehydrated in a graded series of ethanol solutions, before being embedded in Epon resin and undergoing polymerization at 60 °C. Ultrathin sections were obtained using a Leica Ultracut UCT microtome and were stained with 4% uranly acetate with lead citrate before being viewed under a JEOL JEM1010 microscope at 80 kv accelerating voltage.

For the immunogold labeling experiments, cells transfected with V5-BAHD1 expression vector and untransfected cells were fixed with 0.1% glutaraldehyde–4% paraformaldehyde in 0.1 M Sörensen buffer (pH 7.2). Remaining free aldehyde groups were quenched with 0.25% NH_4Cl in 0.1 M Sörensen buffer. Cells were embedded in 4% Agar type 9 diluted in water, stained en bloc with 0.5% uranyl acetate in water, dehydrated according to the progressive lowering of temperature (PLT) method (14), embedded in Lowicryl K4M resin, and polymerized under UV light. After sectioning, as described above, immunolabeling was performed with the Leica EM IGL automated Immunogold labeling system according to the protein A gold method (15), using monoclonal anti-V5 antibody and protein A coupled to 10-nm colloidal gold particles (at Utrecht University Medical Center). Sections were viewed as above.

Protein Purification, Preparation of Nuclear Extracts, GST Pull-Down and Histone Peptide-Binding Assays, IP, and Immunoblotting. To purify GST-tagged proteins, pET41-BAH or pGEX plasmids encoding HP1α or MBD1 were transformed in *Escherichia coli* BL21(DE3), and the GST fusion proteins were produced and purified following standard procedures (Novagen or Amersham Pharmacia Biotech). Histone peptide–binding assays were performed as described previously (16). In brief, 1.0 μg of a biotinylated histone peptide (12–403, 12–405, 12–407, 12–408, 12–565, or 12–568; Millipore) or a biotinylated positively charged control KK-peptide (KPKKAAPKKK-biotin; Eurogentec) was incubated with 1 μg of protein in binding buffer [50 mM Tris-HCl (pH 7.5), 300 mM NaCl, 0.1% Nonidet P-40, 1 mM PMSF, plus protease inhibitors] overnight at 4 °C with rotation. After a 1-h incubation with avidin beads (Amersham) and extensive washing, bound proteins were analyzed by SDS/PAGE and Western blotting with anti-BAHD1 or anti-HP1α antibodies. For pull-down assays, 100 μL of a 50% slurry of gluthatione Sepharose 4B beads (Amersham) was mixed with each bacterial lysate for 4 h at 4 °C. The resin was collected and washed 3 times with supplemented PBS and then resuspended in 1 mL of binding buffer [50 mM Tris-HCl (pH 7.5), 150 mM NaCl, 0.5 mM EDTA, 0.5% Nonidet P-40] supplemented with protease inhibitor mixture. The amounts of GST fusion proteins were estimated by either Western blot analysis or Coomassie brilliant blue staining for normalization of quantities used in the pull-down assay. Nuclear extracts from 4×10^7 HEK293 cells transfected or not transfected with pcV5-BAHD1 or pcV5-CFP expression vectors were purified using a Active Motif Nuclear Extraction Kit following the manufacturer's instructions. Here 50 μL of purified nuclear extract including V5-BAHD1 or V5-CFP was mixed with appropriate quantities of GST fusion protein resin in supplemented binding buffer overnight at 4 °C. The beads were then washed twice with the same binding buffer and once with binding buffer without the protease inhibitor mixture. Then 20 μL of SDS/PAGE loading buffer was added, and the mixture was boiled for 6 min. After centrifugation at 2500× *g* for 5 min, 15 μL of the supernatant was subjected to SDS/PAGE and Western blot analysis using Hybond membranes (Amersham) and a Pierce detection kit. IP experiments were performed with the Active Motif Nuclear Complex Co-IP Kit. For each IP, 500 μg of nuclear extracts prepared following the manufacturer's instructions was diluted in low-IP buffer supplemented with 150 mM NaCl and 0.2% detergent, and then incubated with 5 μg of V5 mAb or mouse IgG. Complexes were recovered with 50 μL of magnetic beads (Dynabeads protein G; Invitrogen), washed 5 times in IP buffer, resuspended in 20 μL of sample buffer 2X, and processed for SDS/PAGE and transfer on PVDF membranes. Detection was performed using Amersham ECL+ chemiluminescence reagents.

Luciferase Reporter Assays. HEK293 cells were transfected with the indicated luciferase reporters (100 ng/24-well plate) together with GAL expression constructs, as shown in Fig. S1. When required, the total amount of DNA was kept constant with a pCDNA vector (Invitrogen). pCMV-Renilla luciferase (2 ng/24-well plates; Promega) was included in all transfections to control for transfection efficiency. When the MMTV-luc reporter was used, cells were treated with dexamethasone 1 μM overnight before protein extraction. Firefly and Renilla luciferases were

measured at 48 h after transfection using Promega luciferase assay reagents according to the manufacturer's instructions. Protein content was measured using Bradford reagent (Bio-Rad). Luminometer readings were expressed as arbitrary units and expressed as the percentage of an appropriate control, as indicated in Fig. S1. All transfection experiments were carried out in triplicate wells and repeated 2 or 3 times.

Microarray Analysis. Total RNA from cells transfected for 72 h with siRNA BAHD1 or siRNA control was extracted and purified using the Qiagen RNeasy Kit. The quality of RNAs and cRNAs was monitored on Agilent RNA Nano LabChips. RT-PCR on 5 μg of total RNA using oligo(dT) primers and in vitro transcription of the cDNA in presence of biotin were done using a Affymetrix GeneChip Amplification One-Cycle Target Labeling Kit according to standard protocols. Fragmented, biotin-labeled cDNA samples were hybridized on Array Type GeneChip Human Genome U133Plus 2.0. For each condition, 3 biological replicates were hybridized. Data and statistical analysis were performed as described previously (17), with the following modifications. GeneChip Operating Software (GCOS; Affymetrix) was used to generate the report (RPT) files containing the hybridization quality control (QC) metrics for each GeneChip of the experimental design. Thereafter, hybridization quality was assessed by uploading all of the RPT files with the AffyGCQC Web-based interface (Osorio) to visualize the Affymetrix-recommended metrics with a graphical representation and to identify potential deviating measures with an outlier detection statistical test. GCOS software determines a detection call (absence/presence) using Wilcoxon statistics for each probe set. The fold changes of the differentially expressed genes after *P* value adjustment (threshold, .05) were analyzed by filtering the data set with a threshold of Log2 ratio = 0.5 (1.4-fold change). Additional filtering was applied so that "unknown" transcripts, redundant probe sets, and genes called "absent" in all 6 chips were removed. The data have been deposited in NCBI's Gene Expression Omnibus and are accessible through GEO series accession number GSE16097 (http://www.ncbi.nlm.nih.gov/geo/query/acc.cgi?acc = GSE16097).

Data were uploaded in the Ingenuity Pathways Analysis software (www.ingenuity.com). Genes from the data set that were associated with networks, biological functions, and/or diseases in the Ingenuity Pathways Knowledge Base were considered for the analysis. For generation of networks, genes of the data set, called focus genes, were overlaid onto a global molecular network developed from information contained in the Ingenuity Pathways Knowledge Base. Networks of these focus genes were then algorithmically generated based on their connectivity. The functional analysis identified the most significant biological functions and/or diseases to the data set. Fisher's exact test was used to calculate a *P* value determining the probability that each biological function and/or disease assigned to that data set was due to chance alone.

RNA Isolation, RT-PCR, and Analysis of Transcript Levels. RNA from cells was extracted using the Qiagen RNeasy Kit. cDNA preparation and qPCR assays were carried out by Cogenics (www.cogenics.com), as follows. RNA was treated with TURBO DNA-free DNase (Applied Biosystems) using 2 μg of total RNA in a volume of 10 μL. cDNA was obtained by reverse transcription of the DNAse-treated RNA using an Applied Biosystems high-capacity cDNA Archive Kit with random primers in a final volume of 50 μL, as recommended by the manufacturer. Primers for SYBR Green chemistry qPCR were designed using a home-made script. Two primer sets per transcript were designed. PCR specificity and efficiency were checked for each primer set using serial dilutions of cDNA. RT-PCR was performed using Power SYBR Green Master Mix–specific primers (400 nM; Applied Biosystems) and cDNA (volume corresponding to 10 ng of total RNA). Taqman Gene expression assays were purchased from Applied Biosystems, and PCR was performed using Applied Biosystems Taqman Universal PCR Master Mix as recommended by the manufacturer. Thermocycling was performed using an Applied Biosystems ABI 7500 Real-Time PCR System. For SYBR Green chemistry and Taqman assays, each measurement was carried out in triplicate. Relative expression quantification was calculated with the 7500 Fast System software using the comparative $\Delta\Delta$Ct method. The internal control gene was *HPRT*, *18S*, or *GAPDH*, depending on the experiment. The stable expression levels of these housekeeping genes have been validated previously. The range of minimum and maximum fold changes was determined based on the SDs. Statistical significance of the difference in mean expression of genes was evaluated using the Student *t* test; a P value $< .05$ was considered significant. The primers used are listed in Table S5.

Quantification of *IGF2* Relative to *BAHD1* Transcript Levels. To differentially modulate the amount of BAHD1 in cells, HEK293 cells were transfected with V5-BAHD1 for 48 h to increase BAHD1 expression or with *BAHD1* siRNA #1 or #2 for 48 h or 72 h to differentially decrease BAHD1 expression. Controls were V5-CFP expression vector or siRNA #1 (Ambion #4611), respectively. V5-BAHD1 and V5-CFP transfection efficiencies were evaluated by immunofluorescence using anti-V5 antibody and were found to be ≈70% of total cells. After RNA extraction, the levels of *BAHD1* and *IGF2* transcripts were quantified by qRT-PCR using GAPDH as an internal control, as described earlier.

ChIP and Site-Specific PCR Analysis. We performed ChIP on HEK293 cells transfected for 24 h with V5-BAHD1 or V5-CFP expression vectors. For each vector, the number of transfected cells, evaluated by immunofluorescence using anti-V5 antibody, was ≈70% of total cells. Three independent chromatin preparations per vector, each corresponding to 10^7 cells, were made, immunoprecipitated in duplicate, and quantified in duplicate. Formaldehyde-fixed cells were extracted with 10 mM Tris-HCl (pH 8), 1 mM EDTA, 0.5 mM EGTA, 0.25% (vol/vol) Triton X-100, and protease inhibitors for 5 min on ice. The pellets were then reextracted with TNEN 250 plus inhibitors for 30 min on ice. The resulting pellets were resuspended in 10 mM Tris-HCl (pH 8), 1 mM EDTA, 0.5 mM EGTA, and 0.5% (wt/vol) SDS, and then sonicated to shear chromatin to a final size of 200–500 bp. Extracts were quantified by $DO_{260\ nm}$ to adjust the quantities of material and then diluted to obtain the following buffer composition: 0.1% (wt/vol) SDS, 1% (vol/vol) Triton, 0.1% (wt/vol) sodium deoxycholate, 10 mM Tris-HCl (pH 8), 150 mM NaCl, 1 mM EDTA, 0.5 mM EGTA, and protease inhibitors. IP was carried out overnight at 4 °C with V5 antibodies or control mouse IgG, or with MBD1 or HDAC5 antibodies or control rabbit IgG. The immunocomplexes were recovered with protein G magnetic Dynabeads (Invitrogen) added for 90 min and then washed 5 times in a succession of isotonic and salt buffers (composition available on request) using a magnet system. After a final wash in TE, bound material was eluted by the addition of water containing 10% (wt/vol) Chelex, followed by boiling for 10 min to reverse cross-linking, incubation with proteinase K (100 μg/mL) for 30 min at 55 °C with some shaking, boiling for another 10 min, and finally centrifugation to collect the bound fraction in the supernatant. Aliquots were used for qRT-PCR performed with a Stratagene Mx3005p with SYBR Green kits according to the manufacturer's instructions. The primers were designed using PrimerQuest (www.idtdna.com) with the following advanced settings: Tm = 60 °C ± 1 °C; %GC, 50%; length, 20–25 nucleotides; amplicon size, 75–250 bp. The primer sequences used are given in Table 5. Data were computed as described previously (18). The PCR efficiency (E) was estimated

by sequential dilution of the inputs, followed by amplification with each primer set corresponding to the different amplified genomic regions. The slopes of these curves were then used to calculate the E value as follows: $E = 100 \times (-1 + 10^{(-1/\text{slope})})$. All PCR efficiencies were 90%–100%. Because CpG-rich sequences are difficult to amplify, several pairs of primers were tested by dissociation curve and electrophoresis analysis to select those that gave only a single product by PCR. The values of each PCR for the recruitment of the V5 antibody on chromatin were calculated using the nonimmune IgG antibody on the same chromatin extract as a reference. The measured "cycle thresholds" (Ct) were used to calculate the relative recruitment (R) of the V5 antibodies as follows: RV5 = (1 + E/100)^(CtIgG - CtV5). As control for the specific presence of BAHD1 along the *IGF2* gene in the V5-BAHD1–transfected cells, the same ChIP experiments were conducted on chromatin from cells transfected with plasmid expressing V5-CFP. In addition, the RV5 observed on the CD44 promoter in the V5-BAHD1– and V5-CFP–transfected cells was used to set the reference (RIgG) of the relative recruitment at 1. The CD44 promoter region was used for 2 reasons: (*i*) The expression of this gene was not modified on treatment by the BAHD1 siRNA, and (*ii*) this gene is located on the same chromosome as *IGF2*, and the amplified region lies within a CpG island, as does the *IGF2* P3. The data presented are representative of 3 independent experiments and are averages (± SD) of qPCR replicates.

1. Lisowska-Grospierre B, Fondaneche MC, Rols MP, Griscelli C, Fischer A (1994) Two complementation groups account for most cases of inherited MHC class II deficiency. *Hum Mol Genet* 3:953–958.
2. Cooper HM, Paterson Y (1995) Production of antibodies. *Curr Protocol Immunol* 2:1–9.
3. Miyawaki A, Tsien RY (2000) Monitoring protein conformations and interactions by fluorescence resonance energy transfer between mutants of green fluorescent protein. *Methods Enzymol* 327:472–500.
4. Hoppe A, Christensen K, Swanson JA (2002) Fluorescence resonance energy transfer–based stoichiometry in living cells. *Biophys J* 83:3652–3664.
5. Sadowski I, Ptashne M (1989) A vector for expressing GAL4(1–147) fusions in mammalian cells. *Nucleic Acids Res* 17:7539.
6. Gouilleux F, Sola B, Couette B, Richard-Foy H (1991) Cooperation between structural elements in hormono-regulated transcription from the mouse mammary tumor virus promoter. *Nucleic Acids Res* 19:1563–1569.
7. Fromont-Racine M, Rain JC, Legrain P (1997) Toward a functional analysis of the yeast genome through exhaustive two-hybrid screens. *Nat Genet* 16:277–282.
8. Rain JC, et al. (2001) The protein–protein interaction map of *Helicobacter pylori*. *Nature* 409:211–215.
9. Formstecher E, et al. (2005) Protein interaction mapping: A *Drosophila* case study. *Genome Res* 15:376–384.
10. Altschul SF, et al. (1997) Gapped BLAST and PSI-BLAST: A new generation of protein database search programs. *Nucleic Acids Res* 25:3389–3402.
11. Rual JF, et al. (2005) Towards a proteome-scale map of the human protein–protein interaction network. *Nature* 437:1173–1178.
12. Bierne H, et al. (2005) WASP-related proteins, Abi1 and Ena/VASP, are required for *Listeria* invasion induced by the Met receptor. *J Cell Sci* 118(Pt 7):1537–1547.
13. Rosset A, Spadola L, Pysher L, Ratib O (2006) Informatics in radiology (infoRAD). Navigating the fifth dimension: Innovative interface for multidimensional multimodality image navigation. *Radiographics* 26:299–308.
14. Carlemalm E, Villiger W, Hobot JA, Acetarin JD, Kellenberger E (1985) Low-temperature embedding with Lowicryl resins: Two new formulations and some applications. *J Microsc* 140(Pt 1):55–63.
15. Slot JW, Geuze HJ, Gigengack S, Lienhard GE, James DE (1991) Immuno-localization of the insulin regulatable glucose transporter in brown adipose tissue of the rat. *J Cell Biol* 113:123–135.
16. Shi X, et al. (2006) ING2 PHD domain links histone H3 lysine 4 methylation to active gene repression. *Nature* 442:96–99.
17. Hamon MA, et al. (2007) Histone modifications induced by a family of bacterial toxins. *Proc Natl Acad Sci USA* 104:13467–13472.
18. Pfaffl MW (2001) A new mathematical model for relative quantification in real-time RT-PCR. *Nucleic Acids Res* 29:e45.
19. Bracken AP, Dietrich N, Pasini D, Hansen KH, Helin K (2006) Genome-wide mapping of Polycomb target genes unravels their roles in cell fate transitions. *Genes Dev* 20:1123–1136.
20. Hediger F, Gasser SM (2006) Heterochromatin protein 1: Don't judge the book by its cover! *Curr Opin Genet Dev* 16:143–150.
21. Grewal SI, Jia S (2007) Heterochromatin revisited. *Nat Rev Genet* 8:35–46.
22. Wade PA (2001) Methyl CpG binding proteins: Coupling chromatin architecture to gene regulation. *Oncogene* 20:3166–3173.
23. Zhang CL, McKinsey TA, Olson EN (2002) Association of class II histone deacetylases with heterochromatin protein 1: Potential role for histone methylation in control of muscle differentiation. *Mol Cell Biol* 22:7302–7312.
24. Klose RJ, Bird AP (2006) Genomic DNA methylation: The mark and its mediators. *Trends Biochem Sci* 31:89–97.
25. Fujita N, et al. (2003) Methyl-CpG binding domain 1 (MBD1) interacts with the Suv39h1–HP1 heterochromatic complex for DNA methylation–based transcriptional repression. *J Biol Chem* 278:24132–24138.
26. Fujita N, et al. (2003) MCAF mediates MBD1-dependent transcriptional repression. *Mol Cell Biol* 23:2834–2843.
27. Tai HH, et al. (2003) CHD1 associates with NCoR and histone deacetylase as well as with RNA splicing proteins. *Biochem Biophys Res Commun* 308:170–176.
28. Rippe K, et al. (2007) DNA sequence- and conformation-directed positioning of nucleosomes by chromatin-remodeling complexes. *Proc Natl Acad Sci USA* 104:15635–15640.
29. Lemercier C, et al. (2000) mHDA1/HDAC5 histone deacetylase interacts with and represses MEF2A transcriptional activity. *J Biol Chem* 275:15594–15599.
30. Huang EY, et al. (2000) Nuclear receptor corepressors partner with class II histone deacetylases in a Sin3-independent repression pathway. *Genes Dev* 14:45–54.
31. Yang L, et al. (2002) Molecular cloning of ESET, a novel histone H3-specific methyltransferase that interacts with ERG transcription factor. *Oncogene* 21:148–152.
32. Li H, et al. (2006) The histone methyltransferase SETDB1 and the DNA methyltransferase DNMT3A interact directly and localize to promoters silenced in cancer cells. *J Biol Chem* 281:19489–19500.
33. Ichimura T, et al. (2005) Transcriptional repression and heterochromatin formation by MBD1 and MCAF/AM family proteins. *J Biol Chem* 280:13928–13935.
34. Allis CD, et al. (2007) New nomenclature for chromatin-modifying enzymes. *Cell* 131:633–636.
35. Colland F, et al. (2004) Functional proteomics mapping of a human signaling pathway. *Genome Res* 14:1324–1332.
36. Rohr O, Aunis D, Schaeffer E (1997) COUP-TF and Sp1 interact and cooperate in the transcriptional activation of the human immunodeficiency virus type 1 long terminal repeat in human microglial cells. *J Biol Chem* 272:31149–31155.
37. Maeda T, Chapman DL, Stewart AF (2002) Mammalian vestigial-like 2, a cofactor of TEF-1 and MEF2 transcription factors that promotes skeletal muscle differentiation. *J Biol Chem* 277:48889–48898.
38. Jeronimo C, et al. (2007) Systematic analysis of the protein interaction network for the human transcription machinery reveals the identity of the 7SK capping enzyme. *Mol Cell* 27:262–274.
39. Valdez BC, Yang H, Hong E, Sequitin AM (2002) Genomic structure of newly identified paralogue of RNA helicase II/Gu: Detection of pseudogenes and multiple alternatively spliced mRNAs. *Gene* 284:53–61.
40. Venables JP, et al. (1999) T-STAR/ETOILE: A novel relative of SAM68 that interacts with an RNA-binding protein implicated in spermatogenesis. *Hum Mol Genet* 8:959–969.
41. Fuks F, Hurd PJ, Deplus R, Kouzarides T (2003) The DNA methyltransferases associate with HP1 and the SUV39H1 histone methyltransferase. *Nucleic Acids Res* 31:2305–2312.
42. Lehnertz B, et al. (2003) Suv39h-mediated histone H3 lysine 9 methylation directs DNA methylation to major satellite repeats at pericentric heterochromatin. *Curr Biol* 13:1192–1200.
43. Smallwood A, Esteve PO, Pradhan S, Carey M (2007) Functional cooperation between HP1 and DNMT1 mediates gene silencing. *Genes Dev* 21:1169–1178.
44. Vire E, et al. (2006) The Polycomb group protein EZH2 directly controls DNA methylation. *Nature* 439:871–874.
45. Sanchez C, et al. (2007) Proteomics analysis of Ring1B/Rnf2 interactors identifies a novel complex with the Fbxl10/Jhdm1B histone demethylase and the Bcl6 interacting corepressor. *Mol Cell Proteomics* 6:820–834.
46. Sakamoto Y, et al. (2007) Overlapping roles of the methylated DNA-binding protein MBD1 and polycomb group proteins in transcriptional repression of HOXA genes and heterochromatin foci formation. *J Biol Chem* 282:16391–16400.
47. Zhang X, Liu Y (2003) Suppression of HGF receptor gene expression by oxidative stress is mediated through the interplay between Sp1 and Egr-1. *Am J Physiol Renal Physiol* 284:F1216–F1225.
48. Firulli BA, Hadzic DB, McDaid JR, Firulli AB (2000) The basic helix-loop-helix transcription factors dHAND and eHAND exhibit dimerization characteristics that suggest complex regulation of function. *J Biol Chem* 275:33567–33573.
49. Morin S, Pozzulo G, Robitaille L, Cross J, Nemer M (2005) MEF2-dependent recruitment of the HAND1 transcription factor results in synergistic activation of target promoters. *J Biol Chem* 280:32272–32278.
50. Maeda T, Gupta MP, Stewart AF (2002) TEF-1 and MEF2 transcription factors interact to regulate muscle-specific promoters. *Biochem Biophys Res Commun* 294:791–797.
51. Pena P, et al. (1999) Activator protein-2 mediates transcriptional activation of the *CYP11A1* gene by interaction with Sp1 rather than binding to DNA. *Mol Endocrinol* 13:1402–1416.
52. Gunther M, Laithier M, Brison O (2000) A set of proteins interacting with transcription factor Sp1 identified in a two-hybrid screening. *Mol Cell Biochem* 210:131–142.
53. Raizis AM, Eccles MR, Reeve AE (1993) Structural analysis of the human insulin-like growth factor-II P3 promoter. *Biochem J* 289(Pt 1):133–139.
54. Rietveld LE, Koonen-Reemst AM, Sussenbach JS, Holthuizen PE (1999) Dual role for transcription factor AP-2 in the regulation of the major fetal promoter P3 of the gene for human insulin-like growth factor II. *Biochem J* 338(Pt 3):799–806.
55. Zhang L, et al. (1998) AP-2 may contribute to IGF-II overexpression in rhabdomyosarcoma. *Oncogene* 17:1261–1270.
56. Robertson G, et al. (2006) cisRED: A database system for genome-scale computational discovery of regulatory elements. *Nucleic Acids Res* 34:D68–D73.

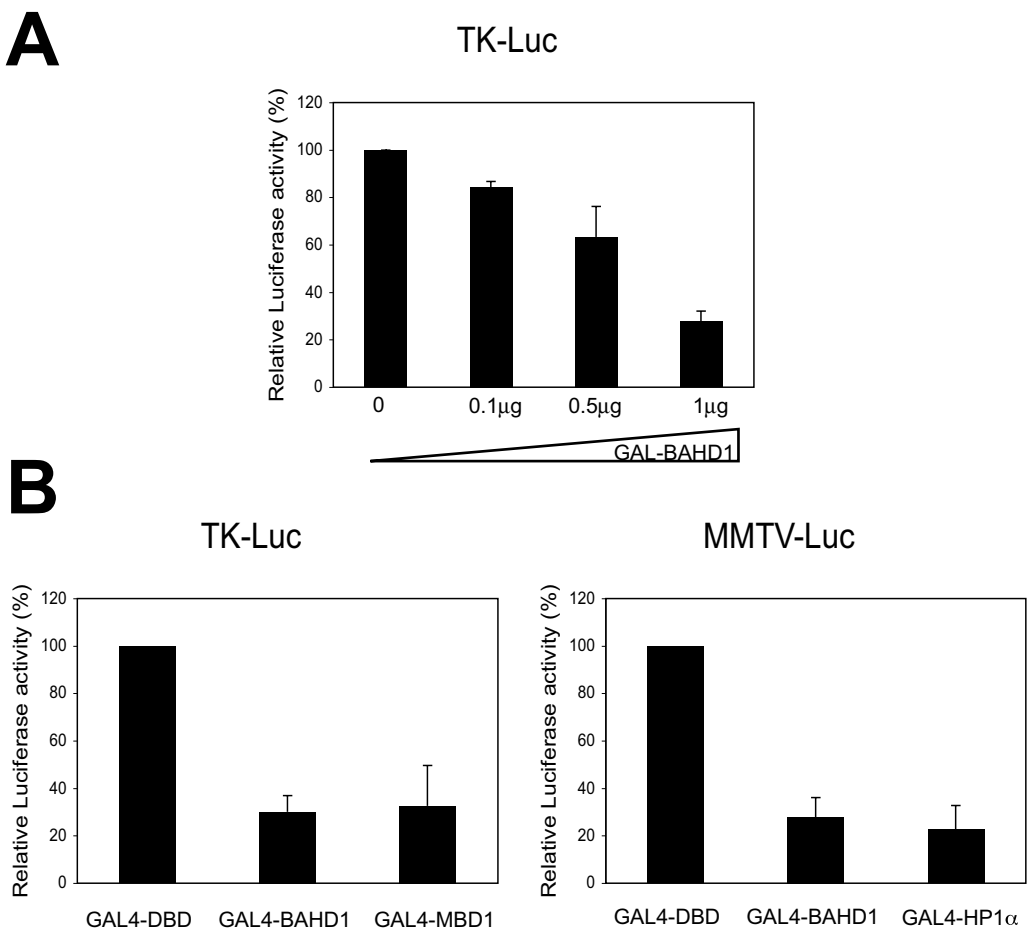

Fig. S1. Transcriptional repression by GAL4-BAHD1. (*A*) BAHD1 acts as a repressor. BAHD1 fused to the DNA-binding domain of GAL4 (GAL4-BAHD1) represses the activity of the thymidine kinase (TK) promoter bearing GAL4 binding sites in a concentration-dependent manner. HEK293 was cotransfected with a GAL4-driven luciferase reporter under the control of TK and increasing amounts of GAL4-BAHD1 expression vector (0.1–1 μg). Total amounts of DNA were kept constant with a pCDNA plasmid. Results are presented as the mean ± SD of 3 transfections, in which the activity of the reporter alone was set to 100%. (*B*) The repressive effects of BAHD1 are comparable to those of MBD1 and HP1α. HEK293 cells were transfected with a reporter containing either TK or the mouse mammary tumor virus (MMTV) promoters driving luciferase (TK-Luc or MMTV-Luc; 0.1 μg) together with GAL4-DBD, GAL4-BAHD1, GAL4-HP1α, or GAL4-MBD1 expression constructs (0.5 μg). MMTV promoter was stimulated by dexamethasone 1 μM overnight before protein extraction. pCMV-Renilla luciferase (2 ng) was included in all transfections to control for transfection efficiency. Luciferase expression was measured after 48 h. Results are presented as the mean ± SD of 3 transfections, in which the activity of reporters in the presence of the GAL4 control expression vector (GAL4-DBD) is set to 100%. Independent experiments repeated at least twice give similar results. Detailed experimental procedures are described in SI *Materials and Methods*.

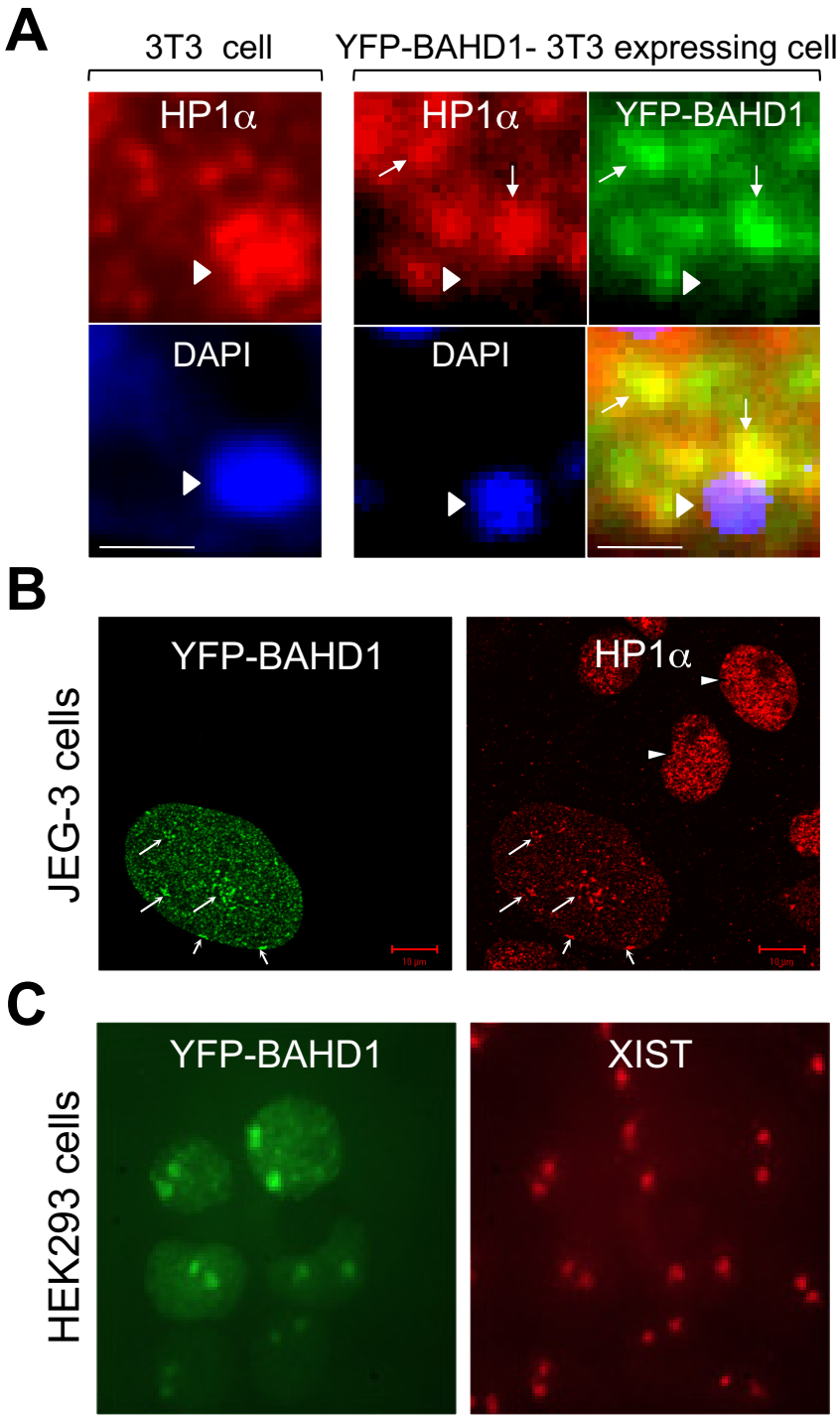

Fig. S2. Characterization of BAHD1-associated heterochromatin foci. (*A*) YFP-BAHD1 recruits HP1α in mouse fibroblasts. Shown are high-magnification images of 3T3 fibroblast nuclei untransfected (*Left*) and expressing YFP-BAHD1 (*Right*) (see Fig. 2). HP1α accumulated at a chromocenter stained with DAPI (triangle) in the untransfected cell. In contrast, HP1α no longer colocalized with DAPI at the chromocenter in the YFP-BAHD1–expressing cell, being relocated at YFP-BAHD1 foci (arrows). HP1α colocalization with YFP-BAHD1 appears in yellow in the merged image. (Scale bar: 1 μm.) (*B*) Relocalization of HP1α at YFP-BAHD1 foci in epithelial JEG3 cells. A confocal image of JEG3 cells transfected with the YFP-BAHD1 expression vector and labeled with anti-HP1α is shown. Arrows indicated the focused accumulation of HP1α at BAHD1-associated heterochromatin. Dispersed localization of HP1α throughout nuclei of surrounding untransfected cells is indicated by triangles. (Scale bar: 10 μm.) (*C*) Exogenous BAHD1 is recruited at the Xi chromosomes. Several HEK293 cells transfected for 24 h with the vector expressing YFP-BAHD1 are shown. YFP-BAHD1 localizes to the Xi chromosome, as detected by RNA FISH using a *Xist* probe.

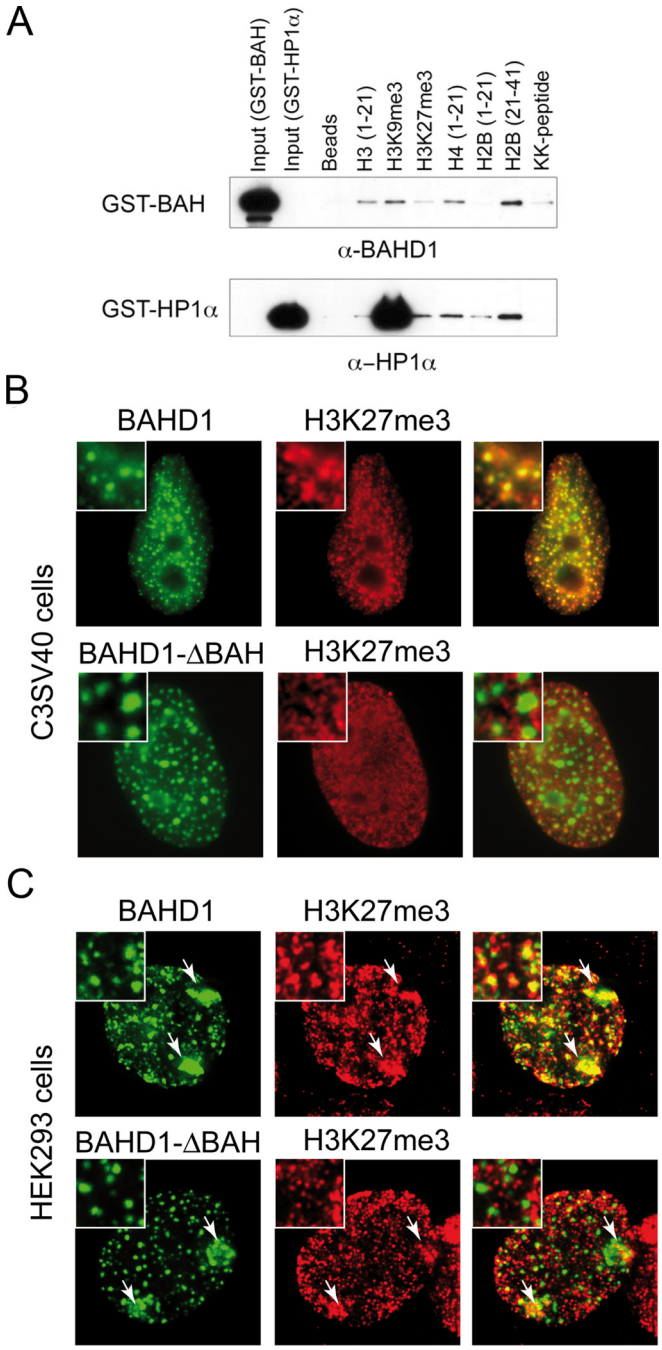

Fig. S3. The BAH domain does not bind H3K27me3 in vitro but is required for BAHD1 targeting to H3K27me3 in vivo. (*A*) Western blot analysis of histone peptide–binding assays with the indicated GST fusion proteins and biotinylated peptides. The BAHD1 BAH domain does not specifically bind the H3K27me3 peptide, whereas GST-HP1 strongly interacts with the H3K9me3 peptide. A weak unspecific binding of both GST-BAH and GST-HP1 to biotinylated peptides was observed as a probable background of this assay, as shown with control histone H4- or H2B-derived peptides or KK-peptide, which has a similar charged amino acid content as the H3 tail. (*B* and *C*) BAHD1-ΔBAH nuclear foci in C3SV40 cells (*B*) or in HEK293 cells (*C*) were not stained with H3K27me3 antibodies, in contrast to BAHD1 foci. In HEK293 cells, BAHD1-ΔBAH is still targeted at the Xi chromosome, where it colocalizes with H3K27me3 (arrows). Squared regions show nuclear foci at higher magnification.

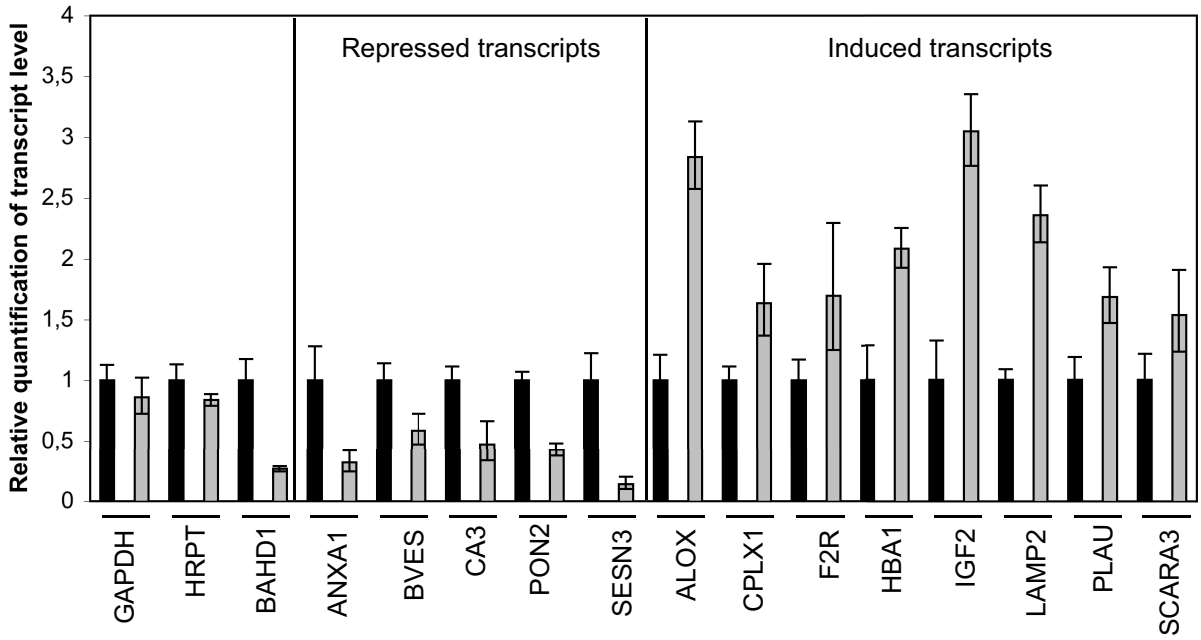

Fig. S4. Validation of gene expression changes on BAHD1 depletion by qRT-PCR for a selection of genes. mRNA was prepared from HEK293 cells transfected for 72 h with control siRNA (black) or BAHD1 siRNA (gray). The experiments were performed independent of the gene expression array experiments on a selection of repressed and induced genes. *GAPDH* and *HRPT* were used as controls for genes not altered in BAHD1 KD cells, with RNA normalization using 18S. Normalization using *HRPT* gave similar results. Depletion of *BAHD1* was quantified in each experiment. The results are representative of 3 independent experiments.

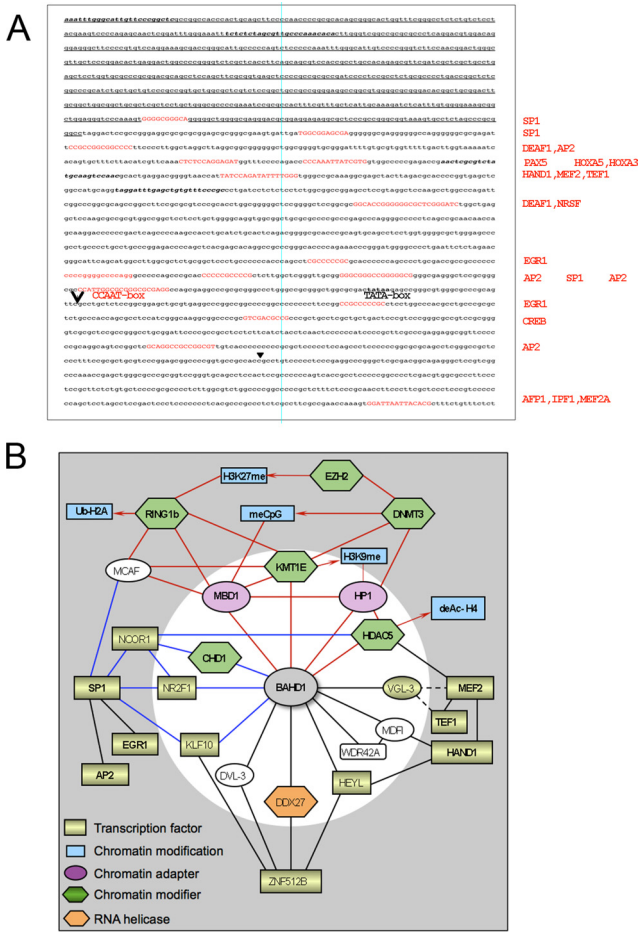

Fig. S5. BAHD1 connects chromatin modifiers to DNA-binding transcription factors. (*A*) A sequence of *IGF2* upstream of P3 showing putative binding sites for transcription factors. The sequence is from the Ensembl database (ID: ENSG00000167244). Consensus sequences for transcription factors (*Right*), indicated in red, are from Raizis et al. (53), Rietveld et al. (54), and the human promoter-based cisRED database (Human 9 database; http://www.cisred.org) (56). The arrow and triangle indicate the transcription start sites mapped by Raizis et al. (53) and predicted in Ensembl (ID: ENST00000381406), respectively. The sequence of primers used to amplify P3b and P3c fragments are in bold italics. The underscored sequence indicates the position of the first exon of *IGF2AS* on the opposite strand (Ensembl database; ID ENST00000381361). Binding of AP2 to *IGF2* P3 has been reported previously (53, 55). (*B*) A network highlighting possible interactions among BAHD1, chromatin regulatory proteins, and *IGF2* transcription factors. Direct BAHD1 interactors identified in yeast two-hybrid screening (within the white circle) were connected to partners (in the gray square) using the Ingenuity and HRPD knowledge bases. Proteins are represented as nodes, and protein–protein interactions between 2 nodes are represented as edges (lines). Arrows indicate formation of chromatin modifications. All edges and arrows are supported by experimental work described by at least one reference in the literature. Blue lines connect components that bridge BAHD1 to SP1. Red lines connect components involved in chromatin condensation, and red arrows indicate chromatin modification activities, generating H3 methylation at K9 (H3K9me) or at K27 (H3K27me), H4 deacetylation (deAc-H4), H2A ubiquitylation (Ub-H2A), or CpG methylation (meCpG). Dashed lines indicate potential interactions (37). Protein names, functions, and references are given in Table S1.

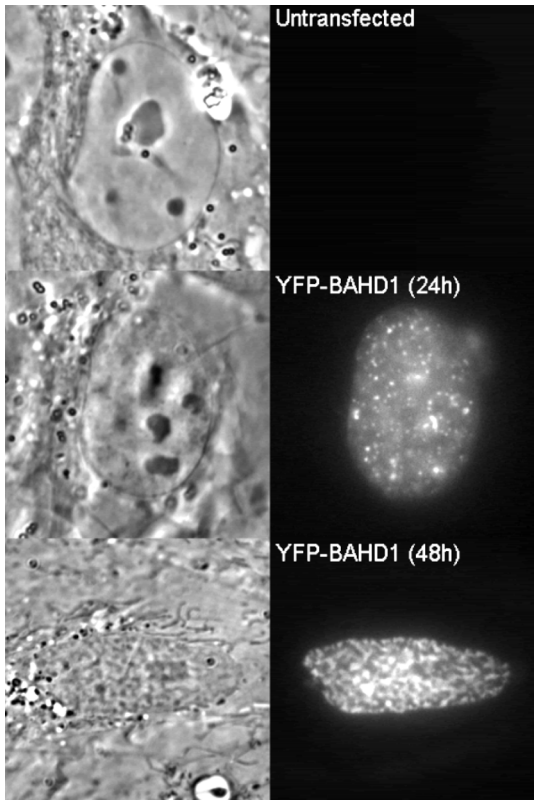

Movie S1. Increasing BAHD1 expression stimulates the formation of phase-dense nuclear structures in living cells. C3SV40 living cells untransfected or transiently transfected with plasmid encoding YFP-BAHD1 (for 24 h or 48 h) were placed under a microscope at 37 °C, and image series were collected every 30 s for 30 min. After a short (24 h) transfection time, YFP-BAHD1 localized in the nucleus as small dispersed and dynamic foci that increased in size on increased transfection time (48 h) to form static larger structures, visible in phase contrast as patches of dense material, and in electron microscopy as heterochromatin areas (see Fig. 1). (Scale bar: 10 μm.)

Movie S1 (AVI)

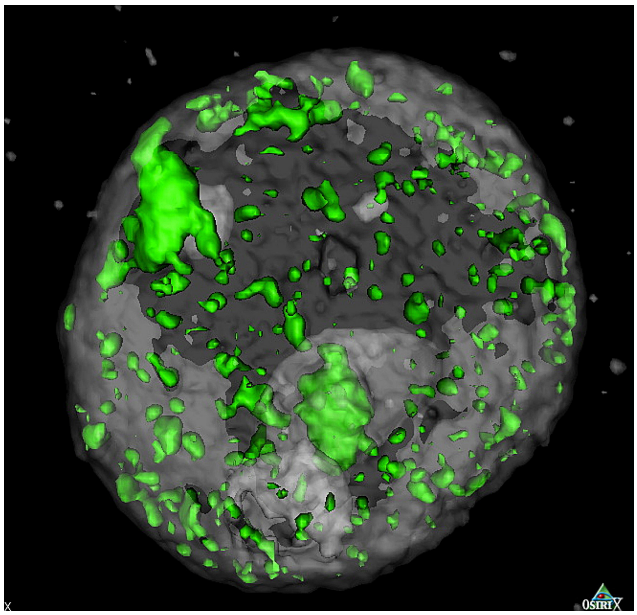

Movie S2. Spatial localization in 3D of exogenous V5-BAHD1 in a HEK293 cell nucleus. V5-BAHD1 accumulated at the 2 Xi chromosomes located at the nuclear periphery and at foci dispersed in the nucleus in a HEK293 cell. Deconvoluted confocal series images of cross-sections of a cell transfected with V5-BAHD1 expression vector were reconstructed in 3D using OsiriX software. V5-BAHD1 is labeled in green, and the nucleus volume is labeled in gray.

Movie S2 (AVI)

Other Supporting Information Files

Table S1

Table S2

Table S3

Table S4

Table S5